ARCES Observations of the TESS Circumbinary Planet TIC 172900988b

Robert F. Wilson (U.Virginia), Veselin Kostov (NASA/Goddard) , Jerome Orosz (SDSU), Steven R. Majewski (U.Virginia)

Abstract: Kostov et al. (2021) report the discovery of the first transiting circumbinary planet, detected from a single sector of TESS data. ARCES observations played a role in helping to establish the parameters of the system. We briefly present an overview of this interesting planetary system and then discuss the challenges encountered in analyzing ARCES data to derive accurate radial velocities for this project.

Overview of the Circumbinary Planet System

We report the first discovery of a transiting circumbinary planet detected from a single sector of TESS data. During Sector 21, the planet TIC 172900988b transited the primary star and then 5 days later it transited the secondary star. The binary is itself eclipsing, with a period of $P \approx 19.7$ days and an eccentricity of $e \approx 0.45$. Archival data from ASAS-SN, Evryscope, KELT, and SuperWASP reveal a prominent apsidal motion of the binary orbit, caused by the dynamical interactions between the binary and the planet. A comprehensive photodynamical analysis of the TESS, archival and follow-up photometric and spectroscopic data yields stellar masses and radii of $M_1 = 1.2377 \pm 0.0009$ $M_\odot$ and $R_1 = 1.3827 \pm 0.0025$ $R_\odot$ for the primary and $M_2 = 1.2021 \pm 0.0008$ $M_\odot$ and $R_2 = 1.3141 \pm 0.0013$ $R_\odot$ for the secondary. The radius of the planet is $R_3 = 11.07 \pm 0.47$ $R_\oplus$ (1.009 ± 0.043 R_{Jup}). The planet's mass and orbital properties are not uniquely determined—there are six solutions with nearly equal likelihood. Specifically, we find that the planet's mass is in the range of $822 \leq M_3 \leq 981 M_\oplus$ ($2.59 \leq M_3 \leq 3.09 M_{Jup}$), while its orbital period could be 188.8, 190.4, 194.0, 199.0, 200.4, or 204.1 days and the eccentricity is between 0.02 and 0.09. At V=10.141, the system is accessible for high-resolution spectroscopic observations, e.g., Rossiter-McLaughlin effect and transit spectroscopy.

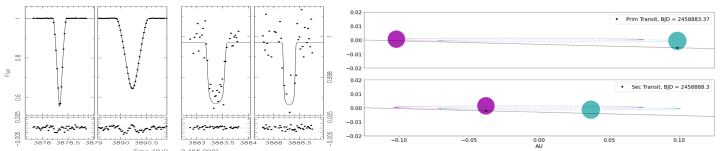

Above, from left to right: (left four panels, all shown with best-fit model and residuals of the fit) the TESS data for the primary eclipse, secondary eclipse, planet transit of the primary, and planet transit of the secondary, and (right panels) the configuration of the system at the times of the two TESS transits.

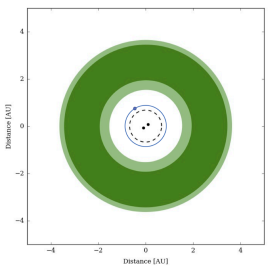

Right: Face on view of the system geometry, showing conservative (dark green) and optimistic (light green) habitable zones of the TIC 1729 system. The orbit of the CBP is shown in blue. The dashed black circle represents the planet's critical instability orbit.

Radial Velocity (RV) Follow-up of the TIC 172900988 System: ARCES Versus Other Spectrographs

To aid in characterizing the architecture of this system, ground-based photometry of additional transits as well as RV monitoring of the binary were obtained. We collected four spectra using the R = 60,000 Tull Coude spectrograph (Tull et al. 1995) on the McDonald 2.7 m telescope, four spectra with the R = 44,000 Tillinghast Reflector Echelle Spectrograph (TRES, Szentgyorgyi & Furesz 2007; Buchave et al. 2010) on the Whipple 1.5m, eight spectra with the high resolution (2 m/s stability) SOPHIE exoplanet-finding spectrograph (Perruchot et al. 2008) on the 1.9m at Observatoire de Haute-Provence, and two spectra with the R ~ 32,500 ARCES on the ARC 3.5-m. These data provide an opportunity to compare the performance of the ARCES against other high resolution instruments, and demonstrate some particular challenges ARCES data impose on this kind of RV monitoring work relative to data from comparable instruments.

All spectra were reduced in the traditional way. For example, for the ARCES spectra quartz and ThAr lamps were taken for flux and wavelength calibration. Images were bias and dark subtracted, and spectral extraction, initial wavelength calibration, and normalization were performed using custom Python routines. An initial wavelength solution was performed by fitting a 4th-order polynomial for each order and then refined with a two dimensional dispersion solution using the IRAF `echelle` package. To extract the RVs of each star from the spectra we used the "broadening function" (BF) technique (Rucinski 1992, 2002). A high *S/N* spectrum of a slowly rotating star is used as a template for the BF analysis; twilight sky was used for the ARCES template. The BFs were extracted separately for each order. Representative BFs are shown for each instrument below (left).

The ARCES spectra were the most challenging from which to extract RVs. We used 51 orders from ~4000 to ~6700 Å (skipping orders with strong telluric absorption). After BFs were found, it was apparent that there was residual sky contamination (creating an *extra* BF peak at 0 km/s), stronger in bluer orders. Moreover, there is a strong trend in the RVs from individual orders (middle figure below). While the wavelengths of the sky peaks are roughly constant with echelle order, the RVs for both the primary and secondary show an almost linear trend with central wavelengths of the orders. This trend is most likely due to atmospheric refraction at the ~2.5-3 airmasses of the observations, as the 1.6" slit width is larger than the ~1" seeing star image, resulting in a chromatic shift in the stellar line spread function (not seen in the residual sky spectrum, which evenly filled the slit). RVs at the reddest orders are nearly 2 km/s larger than those at blue orders, though ΔRV stays reasonably constant, and can still provide a useful check on the model fit to the system dynamics (lower right).

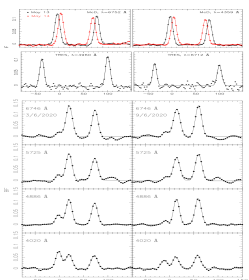

Representative BFs for McDonald (top), TRES (middle) and ARCES data (bottom 8 panels) showing one peak for each binary component, but an extra sky contamination peak for ARCES data.

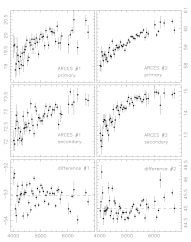

(Left) RVs found for each binary star component from each ARCES order as a function of their central λ, showing clear trends for each star, but at least no λ trend in their RV difference!

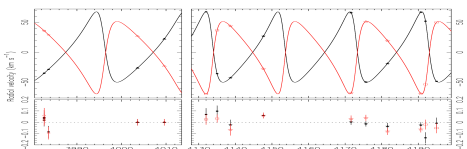

RVs for the primary (black symbols) and secondary (red) stars along with best-fitting model. Data are from McDonald (circles), TRES (squares), SOPHIE (stars), and ARCES (triangles); due to the uncertain calibration, ARCES RVs were left out of final fitting).